

A physically based model for air-lift pumping

Odile François

Department of Geological and Environmental Sciences, Stanford University, Stanford, California

Tyler Gilmore

Pacific Northwest Laboratory, Richland, Washington

Michael J. Pinto and Steven M. Gorelick

Department of Geological and Environmental Sciences, Stanford University, Stanford, California

Abstract. A predictive, physically based model for pumping water from a well using air injection (air-lift pumping) was developed for the range of flow rates that we explored in a series of laboratory experiments. The goal was to determine the air flow rate required to pump a specific flow rate of water in a given well, designed for in-well air stripping of volatile organic compounds from an aquifer. The model was validated against original laboratory data as well as data from the literature. A laboratory air-lift system was constructed that consisted of a 70-foot-long (21-m-long) pipe, 5.5 inches (14 cm) inside diameter, in which an air line of 1.3 inches (3.3 cm) outside diameter was placed with its bottom at different elevations above the base of the long pipe. Experiments were conducted for different levels of submergence, with water-pumping rates ranging from 5 to 70 gallons/min (0.32–4.4 L/s), and air flow ranging from 7 to 38 standard cubic feet/min (0.2–1.1 m³ STP/min). The theoretical approach adopted in the model was based on an analysis of the system as a one-dimensional two-phase flow problem. The expression for the pressure gradient includes inertial energy terms, friction, and gas expansion versus elevation. Data analysis revealed that application of the usual drift-flux model to estimate the air void fraction is not adequate for the observed flow patterns: either slug or churn flow. We propose a modified drift-flux model that accurately predicts air-lift pumping requirements for a range of conditions representative of in-well air-stripping operations.

1. Introduction

Air-lift pumping operations were recently proposed as a new in situ approach to remove volatile organic compounds (VOCs) from groundwater by in-well air stripping. A special well design, described earlier by *Gvirtzman and Gorelick* [1992, 1993], consisting of air injection into a well at a specific submerged depth, causes water to be lifted and forces groundwater flow toward the well. The water is then reinjected from the same well into the unsaturated zone (above the water table). This creates a circulation cleanup zone around the well. During this process, VOCs are transferred from the contaminated water to the rising air bubbles inside the well. The combined air-lift pumping and in-well air stripping method is applicable to different sites whose groundwater is contaminated with VOCs.

To design the air-lift pumping system, one must have an accurate model which can be used to predict the water flow rate that will occur for a given air injection rate and submergence. Previous models that have been proposed in the literature were found to be deficient in the range of relatively high air flow rates of interest for application of the in-well air stripping system. The failure of the previous models to represent the water flow versus air flow relationship seen in our laboratory data motivated the work presented here. Our con-

cern is not to obtain the maximum water pumping rate or the lowest air to water ratio, which corresponds to a maximum energy efficiency, but to create an efficient stripping system. In such a case, excess air may be required for stripping VOCs compared to a smaller air flow rate required merely for air-lift pumping. Having completed the laboratory and theoretical model development described in this paper, in future work the model will be compared to data from field demonstrations of the in-well air stripping approach for VOC removal. These demonstrations are currently underway.

An experimental mock-up was designed and built at the stripping-well scale, as shown in Figure 1a. The system consists of a well within a well. The outer well has a diameter of 10 inches (25.4 cm) and is 75 feet (22.9 m) long. The inner well is a 70-foot-long (21.3-m-long) pipe with a 5.5-inch (14.0-cm) inside diameter and a 6-inch (15.2-cm) outside diameter which contains a 1.3-inch (3.3-cm) injection air line that can be moved to different heights above the base of the inner well. The water level is adjusted and held constant in the annular space between the inner and outer wells. This maintains a constant submergence or back pressure in the inner well, while water is lifted and discharged at the top at atmospheric pressure. Lift is generated by injecting air at specified flow rates through the air injection line. The range of water flow rates is from 5 to 70 gallons/min (0.32–4.4 L/s), with air injection rates of 7 to 38 standard cubic feet/min (0.2–1.1 m³ STP/min). Submergence ratios, defined as the ratio of submergence of the air line to the total length, were varied from 33 to 70%, which

Copyright 1996 by the American Geophysical Union.

Paper number 96WR00899.
0043-1397/96/96WR-00899\$09.00

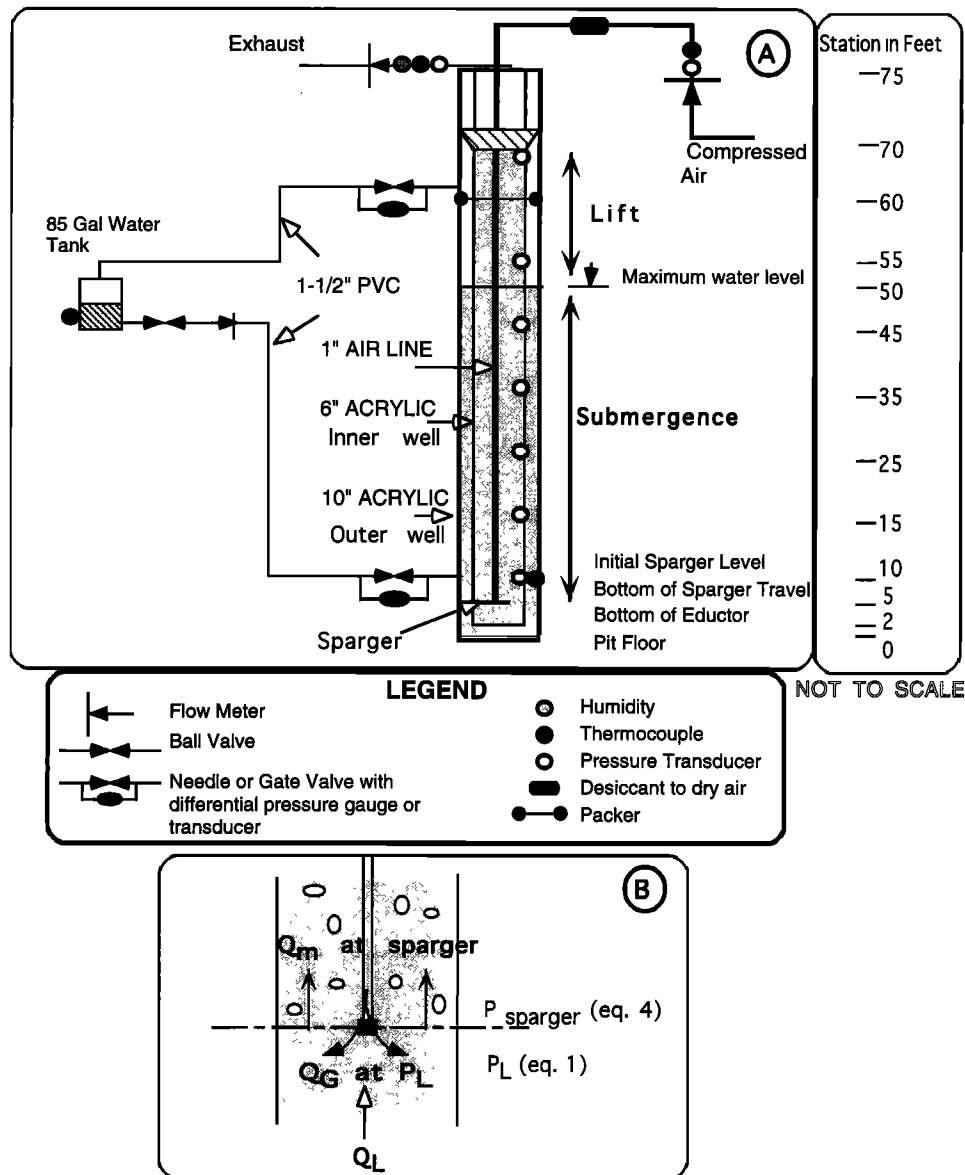


Figure 1. (a) Air-lift pumping lab test apparatus, and (b) detail at the sparger elevation.

corresponds to a range of submergences from 15 to 45 feet (4.6–13.7 m), and lifts from 20 to 35 feet (6.1–10.7 m).

In two-phase flow occurring in a vertical well, four flow patterns can be observed as a function of the air and water superficial velocities. These patterns are illustrated in Figure 2a and are as follows.

1. Bubble flow occurs when dispersed small bubbles flow upward with the liquid.

2. Slug flow is characterized by large gas bubbles, of the diameter of the pipe and of lengths ranging from their diameter to several times this value (Figure 2b). These large bubbles are referred to as gas slugs or Taylor bubbles. Each space between these large bubbles is mostly liquid filled but contains numerous small gas bubbles and is referred to as a liquid slug. Between the Taylor bubbles and the pipe wall, liquid flows downward in the form of a thin falling film [Taitel *et al.*, 1980].

3. Churn flow, which is similar to slug flow but with a more chaotic and disordered flow pattern, may occur at higher air

injection rates. It is an intermediate flow pattern between slug flow and annular flow [Hewitt and Jayanti, 1993].

4. Annular flow occurs when the liquid phase flows upward as a film along the pipe wall, and the gas phase flows as a separate phase in the center of the well.

We report the results of six experiments. The experiments showed that the air-lift operations led to either slug flow or churn flow, depending on the rate of air injection. Whereas the transition criteria between slug and churn flow have been investigated by different authors [Taitel *et al.*, 1980; Bilicki and Kestin, 1987; Jayanti and Hewitt, 1992], the existence of the churn flow pattern as a separate and distinct flow pattern remains problematic [Mao and Dukler, 1993]. Therefore the theoretical approach we followed will be based on the slug flow pattern.

Initially we attempted to use existing air-lift pumping formulas found in the literature to reproduce our laboratory data. No existing model was successful. Therefore we developed a new model. We modeled the air-lift pumping system based on

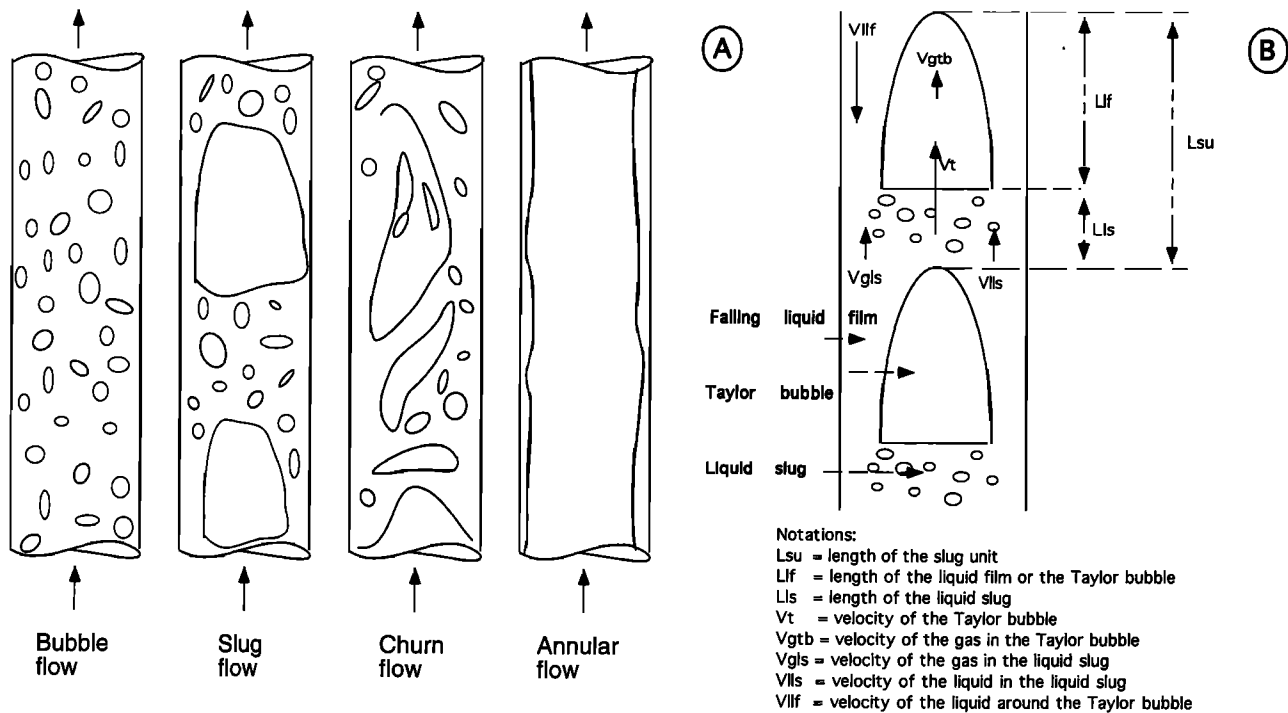


Figure 2. (a) Two-phase flow patterns, after Taitel *et al.* [1980]. (b) Slug flow geometry, after Sylvester [1987].

the two-phase flow equations. This is commonly called the momentum balance approach. Clark and Dabolt [1986] used this approach but neglected the inertial energy effects or acceleration gradient in the differential momentum equation. In our model we take the inertial energy terms into account. Alimonti and Galardini [1992], who also took the inertial energy terms into account, integrated the system of differential equations with simplified inertial energy terms. Therefore their formula is only applicable to small air-lift systems. In our proposed model a direct integration is employed that does not simplify the inertial energy terms and assumes that gas expansion occurs. It was necessary to choose a correlation to express the gas void fraction as a function of the air and water superficial velocities [Zuber and Findlay, 1965; Nicklin *et al.*, 1962]. We modified the correlation of Zuber and Findlay to take into account the presence of the air line and the existence of the two flow patterns: slug and churn. We show that our model can be applied to a broader range of air-lift operation conditions in terms of submergence values and air injection rates than could previous models.

2. Literature Review on Air-Lift Pumping

Several studies have been devoted to model air-lift pumping systems. Their aim is to obtain a simple expression for the relationship between the rate of water flow that is induced by a given air injection rate, for a given submergence. There are three main approaches in the literature. One class of methods is based on empirical correlations. Zenz [1993] found a general correlation (see appendix) using a variety of published air-lift data covering lifts ranging from 5 inches (12.7 cm) to 65 feet (19.8 m) and diameters from 0.5 to 15 inches (1.3–38 cm). However, most of these data are for operations at high water and gas flow rates, and almost no data correspond to our laboratory experiments, which are representative of the conditions required in VOC air stripping systems. The correlation

found by Zenz is applicable for air-lift pumping when air-lift efficiency and maximum capacity are the two important factors (these terms will be defined precisely in section 5). This is not necessarily the case when in-well air stripping is involved because stripping usually employs larger wells and requires air injection rates outside the range of maximum efficiency or capacity.

A second class of methods is based on energy balances assuming a range of values near maximum efficiency [Richardson and Higson, 1962; Shaw, 1920]. The most common is the Ingersoll and Rand formula [Gibbs, 1971, Appendix A]. Zenz [1993, p. 54] noted that this equation is "useful in estimating the yield from air-lift only under conditions of peak theoretical efficiency, but not over the entire range of possible operating conditions." Husain and Spedding [1976] developed a different energy balance theory, which was shown to be valid for small-diameter air-lift systems (less than 0.14 inches (3.5 mm)) and only at high flow rates [Jeelani *et al.*, 1979].

A third class of methods considers an equivalent one-dimensional two-phase flow problem. This approach was first explored by Nicklin [1963]. These models are based on separate continuity and mixture momentum equations [Alimonti and Galardini, 1992; Grandjean *et al.*, 1987; Clark and Dabolt, 1986; Wang and Chen, 1979; Todoroki *et al.*, 1973; Stenning and Martin, 1968]. Many approximations have been introduced to simplify the resulting expressions in order to evaluate the air-lift pumping performance analytically. These approximations limit the range of applications. For example, neglecting the kinetic pressure drops, or simplifying their integration, limits the range of water and gas flow rates to lower values of mixture velocities [Alimonti and Galardini, 1992; Clark and Dabolt, 1986; Reinemann *et al.*, 1990; Stenning and Martin, 1968], and neglecting air compressibility limits the range of total lengths that can be handled [Alimonti and Galardini, 1992; Wang and Chen, 1979; Todoroki *et al.*, 1973; Stenning and Martin, 1968].

In addition to these three main approaches, several particular aspects of air-lift pumping system configurations were studied. Among them is the importance of entrance effects [Nicklin, 1963; Grandjean *et al.*, 1987] and the effects of diffuser design on the efficiency of a small air-lift pumping system [Morrison *et al.*, 1987]. The sensitivity of air-lift pumping performance with respect to the inner well diameter has been examined; Reinemann *et al.* [1990] studied 3- to 35-mm (0.1–1.4 inches) air-lift pumps, and Jeelani *et al.* [1979] tested smaller diameters, ones on the order of 8 mm (0.3 inches) or less. The stability of an air-lift pumping system has been investigated by Ueda and Koizumi [1993] who examined the static and dynamic behavior of the two-phase mixture level in vertical pipes of diameters smaller than 2.6 cm (1.0 inch). In the analysis of Apazidis [1985], only the bubble flow regime was considered. Richardson and Higson [1962] concluded that the fluctuations in the rate of injection of air and in the velocity of the liquid rising in the pipe are dependent on the capacity of the air line. These complementary analyses on entrance effects, stability, and performance are actually secondary in our study. The most important factors are the influence of the flow pattern on model predictions and the assumption that the density of the gas phase is negligible compared to that of the liquid phase.

We have developed a new model valid for slug and churn flow based on a momentum balance. We begin by following the analysis of Clark and Dabolt [1986], in which the flow is considered isothermal and the regime is considered stationary. But as suggested by Alimonti and Galardini [1992], we take into account the kinetic pressure drop. The rigorous solution involves the integration of the entire system of equations. Alimonti and Galardini simplified this integration for the inertial energy terms and therefore limited the range of applicability of their model. We integrate the system without simplifications and also consider the expansion of air bubbles. We neglect the density of air when it is added to that of water as in the case of the formula for the air-water mixture; otherwise we use the equation of state of gas to estimate the air density change with pressure. The average absolute velocity of the gas phase is expressed with the drift-flux model (section 4.3).

Two two-phase flow parameters are then introduced: a coefficient related to the effects of bubble distribution on the velocity profiles and a coefficient describing the drift velocity which is related to the effects of local relative velocity of the two phases. We give their values for different ranges of in-well air stripping injection rates and flow patterns. Our model is valid for short air-lift systems as well as for tall ones, within a range of flow rates that result in either slug flow or churn flow.

3. Air-Lift Pump Design: Experimental Procedure

The principle of air-lift pumping is to inject air in a well, which lightens the column of fluid contained in the well. Water will rise owing to the difference between the weight of the air-water mixture in the well and the weight of the water outside the well. In our laboratory study, whose setup is shown in Figure 1a, air is injected into an inner well while a constant head is maintained outside, in an outer well. To perform this, air is injected through a diffuser or sparger, as shown in Figure 1b, located at the bottom of an air line which is in the center of the inner well.

The key variables that were controlled in the experiments are the air flow rate Q_G , the water pumping rate, Q_L , the

Table 1. Characteristics of the Laboratory System

Description	Variable	Values in Experiments
Inside inner well diameter, cm	d_i	14.2 (5.5 in)
Outside air line diameter, cm	d_o	3.3 (1.3 in)
Total inner well length, m	L_{pipe}	21.3 (70 ft)
Elevation of air diffuser above the bottom of the outer well, m	h	1.5, 7.6 (5, 25 ft)
Fixed submergence	S	
With $h = 1.5$ m (5 feet)		9.1, 10.7, 12.2, 13.7 (30, 35, 40, 45 feet)
With $h = 7.6$ m (25 feet)		4.6, 7.6 (15, 25 feet)
Lift	L	
With $h = 1.5$ m (5 feet)		6.1, 7.6, 9.1, 10.7 (20, 25, 30, 35 feet)
With $h = 7.6$ m (25 feet)		6.1, 9.1 (20, 30 feet)
Water flow rate, L/min	Q_L	19–265 (5–70 gallons/min, 0.7–9.4 standard cubic feet/min)
Gas flow rate, L/min	Q_G	198 to 1076 (52–284 gallons/min, 7–38 standard cubic feet/min)

submergence, S , and the lift, L . The submergence is the level at which air is injected below the water table, or, in our experiments, the level maintained in the outer well. The lift is the height of water rise above the water table. The submergence ratio is a parameter commonly found in air-lift analysis and is defined as the ratio of the submergence to the total length, $\alpha = S/(L + S)$. The air flow rate is measured through a flow meter at the exit of the compressor, and the water-pumping rate is controlled by an entrance valve and measured by a flow meter at the inlet. The characteristics of the laboratory system are listed in Table 1. Figures 3a and 3b are two photographs taken during the laboratory experiments. Figure 3a shows the laboratory well, which extends 50 feet (15.24 m) into an excavated pit and, as shown, goes up 20 feet (6.1 m). Figure 3b shows the leading Taylor bubble rising in the inner well, followed by the liquid slug. One can see the water level in the outer well (defining the submergence) and the air line in the center of the inner well.

The laboratory tests involved two sets of runs, based on the elevation of the air sparger; 5 and 25 feet (1.5 and 7.6 m) above the bottom of the outer well. For a given sparger elevation a range of air flow rates was used, and specified submergence values were maintained. The corresponding water flow rates were measured. For the first set of experiments, in which the sparger was 5 feet (1.5 m) off the bottom, four series of runs were made, characterized by a fixed submergence (30, 35, 40, and 45 feet (9.1, 10.7, 12.2, and 13.7 m)). For the second set of runs, only two submergence values were considered (15 and 25 feet (4.6 and 7.6 m)). In each run the water flow rate varied from 5 to 70 gallons/min (0.32–4.4 L/s), and was measured within ± 1 gallon/min (0.06 L/s). The lift was measured within ± 2 feet (0.6 m). The air flow rate was measured within ± 3 standard cubic feet/min (0.085 m³ STP/min). Measurements of pressure were given through transducers placed along the inner well, and the two-phase flow pattern was recorded on videotapes by cameras placed at various elevations.

4. Air-Lift Pumping Theory

We approach air-lift pumping theory as a two-phase flow problem. We solve the corresponding mixture momentum

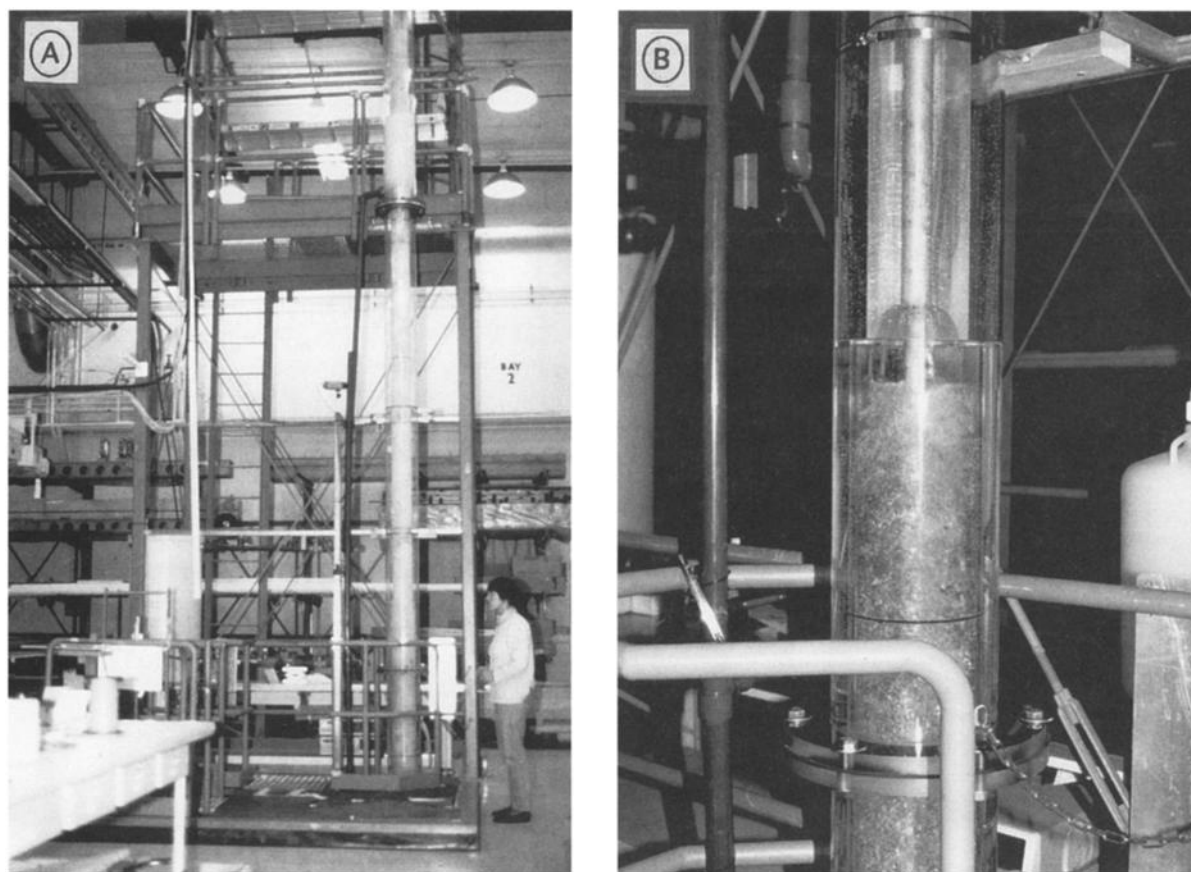


Figure 3. Laboratory experimental setup. The laboratory well extends 50 ft into an excavated pit and goes up 20 feet (6.1 m) (Figure 3a). The flow regime, which occurs in the inner well, is either the slug flow regime which contains a Taylor bubble followed by a liquid slug, or it is the churn flow regime. The first rising Taylor bubble is shown in Figure 3b.

equation in pressure (section 4.2.). Therefore the boundary conditions in pressure must be determined, especially the pressure at the sparger (section 4.1.).

4.1. Expression for the Pressure at the Sparger

Stenning and Martin [1968] provided an excellent starting point to express the pressure at the sparger. With a submergence S and a liquid flow rate Q_L , the pressure below the point of air injection, P_L , is given by Bernoulli's equation:

$$P_L = P_{\text{atm}} + \rho_L g S - \frac{1}{2} \rho_L \left(\frac{Q_L}{A} \right)^2 \quad (1)$$

where P_{atm} is the atmospheric pressure, ρ_L is the water density, g is the gravitational acceleration constant, and A is the inner well cross section. Air is injected through the sparger with the volumetric flow rate, a function of the existing pressure, $Q_G(P_L)$ (Figure 1b). Considering the inner well section at the sparger elevation as a control volume and neglecting the air density changes in this section, volume continuity yields

$$Q_m = A W_{m,\text{sparger}} = Q_G(P_L) + Q_L = Q_G(P_L) + A W_L \quad (2a)$$

or

$$W_{m,\text{sparger}} = W_L \left(1 + \frac{Q_G(P_L)}{Q_L} \right) \quad (2b)$$

$$W_L = \frac{Q_L}{A} \quad (2c)$$

where $W_{m,\text{sparger}}$ is the mixture velocity above the sparger, Q_m is the corresponding flux, and W_L is the superficial velocity of water in the inner well.

Neglecting, in the formulation of the momentum equation, the mass of air and the friction loss of air in the air injection line, we have the pressure above the sparger, P_{sparger} :

$$P_{\text{sparger}} = P_L - \frac{1}{A} [\rho_L Q_L W_{m,\text{sparger}} - \rho_L Q_L W_L] \quad (3)$$

Therefore by rearranging (1), (2), and (3), the pressure is

$$P_{\text{sparger}} = P_{\text{atm}} + \rho_L g S - \frac{1}{2} \rho_L W_L^2 - \frac{\rho_L W_L Q_G}{A} \quad (4)$$

Clark and Dabolt [1986] show that $P_{\text{sparger}} - P_{\text{atm}}$ reduces to the product $\rho_L g S$, which is a good approximation at low water-pumping rates. If higher liquid flow rates are considered, the correction included in (4) as the last two terms must be made.

4.2. Expression for the Total Pressure Drop

The expression for the total pressure drop is shown by *Clark and Dabolt* [1986]. The air-water mixture will discharge at the

location $H = L + S$, at atmospheric pressure, or at any known pressure P_{top} . The overall pressure drop in the inner well is

$$\left(\frac{dP}{dz}\right)_{\text{total}} = \frac{P_{\text{sparger}} - P_{\text{top}}}{L + S} \quad (5)$$

Accurate models have been developed to predict the pressure drop in a slug flow pattern [Caetano *et al.*, 1992a; Barnea, 1990; Sylvester, 1987], based on the hydrodynamic parameters of the slug: air void fractions, lengths, and velocities as denoted by Figure 2a. These models assumed an a priori knowledge of all these parameters. To simplify the prediction of the pressure drop, we use the momentum equation of the gas-liquid mixture:

$$\frac{dP}{dz} + \frac{d(W_m \times W_m \rho_m)}{dz} + g\rho_m + F = 0 \quad (6)$$

The first term is the local pressure drop, where z is the elevation. The second term reflects the acceleration effects neglected by Clark and Dabolt [1986], where ρ_m is the mixture density and W_m is the mixture velocity. The third term corresponds to the gravitational effects due to the weight of the air-water mixture. The last term, F , represents the friction loss per unit pipe length, which we evaluate using the approach of Lockhart and Martinelli [1949]. We need to introduce here D , the frictional pressure loss per unit length of pipe that would occur if the liquid alone were flowing in the inner well:

$$D = \frac{4\rho_L f W_L^2}{2d} \quad (7)$$

where f is the Fanning friction factor and is estimated as a function of the Reynolds number (see appendix). After Clark and Dabolt [1986], we represent the frictional losses F as proportional to D and as a linear function of the cross-sectional average air void fraction, ε :

$$F = D(1 + n\varepsilon) \quad (8)$$

Equation (8) is valid only for air void fractions below 50%, and within this range, the frictional parameter n will be equal to 1.5 [Clark and Dabolt, 1986]. Alimonti and Galardini [1992] have defined F as a nonlinear function of ε , $F = D(1 - \varepsilon)^{-1.75}$. Actually, Clark and Dabolt [1986, p. 59] recognized that "although it is acknowledged that more sophisticated models might be adopted to predict the slug flow pressure loss, these will cause only a small increase in overall accuracy for practical air-lift pump designs, and will prohibit the development of a design equation in closed form."

The air-water mixture density, ρ_m , is also a function of the air void fraction, ε :

$$\rho_m = \varepsilon\rho_G + (1 - \varepsilon)\rho_L \approx (1 - \varepsilon)\rho_L \quad (9)$$

Since the air density ρ_G is small compared to that of water, the air density term is neglected in this equation. However, owing to air expansion along the inner well length, ρ_G is a function of the pressure P . Applying the ideal gas law to air, with ρ_{G_a} as the air mass density at atmospheric pressure, we have the relationship

$$\frac{\rho_G}{\rho_{G_a}} = \frac{P}{P_{\text{atm}}} \quad (10)$$

We use this equation to solve the gas phase continuity equation:

$$\frac{d\rho_G Q_G}{dz} = 0 \quad (11a)$$

where Q_G is the air flow rate and thus will vary with pressure over the height of the inner well. The solution of the liquid phase continuity equation yields a constant water flow rate, Q_L :

$$\frac{d\rho_L Q_L}{dz} = \frac{dQ_L}{dz} = 0 \quad (11b)$$

Finally, the mixture velocity, $W_m = W_G + W_L = (Q_G + Q_L)/A$, is a function of pressure, through the superficial velocity of air, $W_G = Q_G/A$.

Once the air void fraction is known, the momentum equation (6), rearranged through (7)–(11), can be integrated along the inner well. The air flow rate required to pump a certain amount of water is then determined through this integration.

We now present a solution to the momentum equation (6). Readers not interested in this development should skip to section 4.3. By integration of (11a), in which the air mass flow rate is denoted as $G = \rho_G Q_G$, the air superficial velocity W_G is determined as a function of pressure P :

$$W_G = \frac{Q_G}{A} = \frac{GP_{\text{atm}}}{AP\rho_{G_a}} = \frac{M}{P} \quad (12a)$$

Then $W_m = W_L + (M/P)$ and

$$e = \frac{W_G}{C_0 W_m + V_{\text{drift}}} = \frac{M}{C_0 M + P(C_0 W_L + V_{\text{drift}})} = \frac{M}{C_0 M + SP}$$

with

$$S = C_0 W_L + V_{\text{drift}}, \quad M = GP_{\text{atm}}/A\rho_{G_a}$$

Replacing the friction term in (6) with (7) and (8) and the mixture density with (9), the momentum equation (6) becomes

$$0 = \frac{dP}{dz} + \frac{d(W_m^2 \rho_m)}{dz} + g\rho_m + F = \frac{dP}{dz} \left[1 + \left(W_L + \frac{M}{P} \right) \rho_L \left(1 + \frac{M}{P} \right)^2 r_L \frac{MS}{(C_0 M + SP)^2} - 2 \left(W_L + \frac{M}{P} \right) \rho_L \left(1 - \frac{M}{C_0 M + SP} \right) \frac{M}{P^2} \right] + g\rho_L \left(1 - \frac{M}{C_0 M + SP} \right) + D \left(1 + n \frac{M}{C_0 M + SP} \right) \quad (12b)$$

This is a differential equation in pressure that is written as

$$dz + \frac{A_5}{B_5} dP = 0 \quad (12c)$$

with A_5 and B_5 as polynomials of degree 5 in pressure. If

$$R = M\{g\rho_L(C_0 - 1) + D(C_0 + n)\}$$

$$A_5 = (C_0 M + SP)^2 P^3 + (W_L P + M)\rho_L M\{(W_L P + M)SP - 2[SP + (C_0 - 1)M](C_0 M + SP)\} = a_5 P^5 + a_4 P^4 + a_3 P^3 + a_2 P^2 + a_1 P + a_0$$

$$B_5 = (C_0 M + SP)P^3[SP(g\rho_L + D) + R]$$

with

$$\begin{aligned} a_5 &= S^2 \\ a_4 &= 2C_0MS \\ a_3 &= (C_0M)^2 + \rho_L MSW_L(W_L - 2S) \\ a_2 &= -2\rho_L M^2 S[2W_L(C_0 - 1) + S] \\ a_1 &= -\rho_L M^3[2W_L C_0(C_0 - 1) + S(4C_0 - 3)] \\ a_0 &= -2\rho_L M^4 C_0(C_0 - 1) \end{aligned}$$

The decomposition of this polynomial fraction yields

$$\begin{aligned} \frac{A_5}{B_5} &= \frac{1}{g\rho_L + D} + \frac{\delta}{SP(g\rho_L + D) + R} + \frac{\beta}{C_0M + SP} + \frac{\gamma_1}{P} \\ &+ \frac{\gamma_2}{P^2} + \frac{\gamma_3}{P^3} \end{aligned} \quad (12d)$$

where

$$\begin{aligned} \delta &= \frac{C_0M(g\rho_L + D) - R}{g\rho_L + D} + \frac{1}{C_0M(g\rho_L + D) - R} \left[b_2 \right. \\ &\quad \left. + S \left(\frac{g\rho_L + D}{R} \right)^2 \left\{ b_3 - b_4 \left(\frac{g\rho_L + D}{R} \right) \right\} \right] \\ \beta &= \frac{1}{C_0M(g\rho_L + D) - R} \left[-\frac{b_2}{g\rho_L + D} \right. \\ &\quad \left. + \frac{S}{(C_0M)^2(g\rho_L + D)} \left\{ -b_3 + \frac{b_4}{C_0M} \right\} \right] \\ \gamma_1 &= \frac{1}{g\rho_L + D} \left[-b_3 \frac{C_0M(g\rho_L + D) + R}{(RC_0M)^2} \right. \\ &\quad \left. + \frac{b_4}{C_0M(g\rho_L + D) - R} \left\{ \left(\frac{g\rho_L + D}{R} \right)^3 - \left(\frac{1}{C_0M} \right)^3 \right\} \right] \\ \gamma_2 &= \frac{1}{(g\rho_L + D)SRC_0M} \left[b_3 - b_4 \frac{C_0M(g\rho_L + D) + R}{RC_0M} \right] \\ \gamma_3 &= \frac{1}{(g\rho_L + D)S^2} \left[a_2 + \frac{b_4}{RC_0M} \right] \end{aligned}$$

and

$$\begin{aligned} b_2 &= \rho_L MSW_L(W_L - 2S)(g\rho_L + D) \\ b_3 &= (g\rho_L + D)Sa_1 - a_2\{C_0M(g\rho_L + D) + R\} \\ b_4 &= (g\rho_L + D)S^2a_0 - a_2C_0MR \end{aligned}$$

Therefore the integration between the sparger location and the top of the pipe results in

$$\begin{aligned} L + S &= \frac{1}{g\rho_L + D} (P_{\text{sparger}} - P_{\text{top}}) \\ &+ \frac{\delta}{S(g\rho_L + D)} \ln \left[\frac{S(g\rho_L + D)P_{\text{sparger}} + R}{S(g\rho_L + D)P_{\text{top}} + R} \right] \\ &+ \frac{\beta}{S} \ln \left(\frac{C_0M + SP_{\text{sparger}}}{C_0M + SP_{\text{top}}} \right) + \gamma_1 \ln \left(\frac{P_{\text{sparger}}}{P_{\text{top}}} \right) \\ &- \gamma_2 \left(\frac{1}{P_{\text{sparger}}} - \frac{1}{P_{\text{top}}} \right) - \frac{\gamma_3}{2} \left(\frac{1}{P_{\text{sparger}}^2} - \frac{1}{P_{\text{top}}^2} \right) \end{aligned} \quad (12e)$$

Both the water flow rate and the air mass flow rate are present in this equation. This nonlinear equation is solved by successive iterations to predict the air flow rate for a given water flow rate.

It is interesting to note that by setting various coefficients equal to zero in the above equation, we obtain the formula presented by *Clark and Dabolt* [1986], assuming

$$\begin{aligned} b_2 = b_3 = b_4 &= 0 \\ \beta = \gamma_1 = \gamma_2 = \gamma_3 &= 0 \end{aligned}$$

4.3. Expression for the Gas Void Fraction

In this section the expression for the air void fraction is developed. For small wells, or when gas expansion can be ignored, the average gas void fraction $\underline{\varepsilon}$ is given as a function of the submergence ratio α by the approximation

$$\underline{\varepsilon} = \frac{L}{L + S} = 1 - \alpha \quad (13)$$

For the range of lengths of the pipes that we are interested in, the air void fraction cannot be considered as a constant. In order to determine its value in the slug flow regime, different models have been suggested [*Nakazatomi et al.*, 1993]. The most commonly used is the drift-flux model (Zuber and Findlay's drift-flux model), first developed for the bubble flow pattern [*Nicklin et al.*, 1962]. *Zuber and Findlay* [1965] showed that the average absolute velocity of the gas phase, $V_G = W_G/\varepsilon$, is expressed as the sum of a term proportional to the mixture velocity, W_m , and the weighted average drift velocity, V_{drift} . This is the drift-flux model:

$$V_G = \frac{W_G}{\varepsilon} = C_0W_m + V_{\text{drift}} \quad (14)$$

The effects of local relative velocity of the two phases are incorporated in the drift velocity. In bubble flow or churn-turbulent bubble flow, this velocity is given by the terminal rise velocity of bubbles, V_{bs} [*Harmathy*, 1960]:

$$V_{\text{bs}} = 1.53 \left[\frac{\sigma g \Delta \rho}{\rho_L^2} \right]^{1/4} \quad (15)$$

where σ is the air to water surface tension, and $\Delta \rho = \rho_L - \rho_G$. Thus V_{bs} is about 0.24 m/s for the air-water system under normal conditions. The coefficient C_0 reflects the effect of the velocity and air concentration profiles. The concentration profile represents the "variation of the in situ volume fraction of the phases with position. If the phases were uniformly mixed, as in a fine emulsion, the concentration profile would be flat, but in general the phase distribution is not uniform" [*Govier and Aziz*, 1972, p. 384]. If one assumes that the gas phase flows entirely through the channel center, then it can be shown that the flow parameter, C_0 , equals the ratio of the channel center velocity to the cross-sectional average velocity. For turbulent flow this ratio is approximately equal to 1.2. Therefore the usual value selected for C_0 is

$$C_0 = 1.2 \quad (16)$$

Zuber and Findlay [1965] showed that this is only a rough approximation. Its value varies from 1 to 1.5 if the air concentration at the center line is larger than that at the wall, and is less than 1 if the air concentration at the center line is smaller than that at the wall.

Application of the drift-flux model to slug flow is more complicated than in bubble flow because of the different drift velocity of the Taylor bubble compared with that of the small bubbles in the liquid slug. We assume, as is commonly done, that the liquid slugs do not contain any gas bubbles, that the drift velocity is now the rise velocity of a single Taylor bubble in a stagnant liquid, V_{tb} . This velocity V_{tb} is defined as

$$V_{tb} = C_2 \left[\frac{\Delta \rho g d}{\rho_L} \right]^{1/2} \quad (17)$$

in which the value of C_2 , dimensionless velocity, remains constant at 0.345 for many practical systems:

$$C_2 = 0.345 \quad (18)$$

By rearranging (14), in which the air velocity, V_G , is approximated by the Taylor bubble velocity, V_t in Figure 2, the average gas void fraction for the entire slug is approximated using $V_{drift} = V_{tb}$:

$$\varepsilon = \frac{W_G}{C_0 W_m + V_{tb}} = \frac{W_G}{C_0 W_m + C_2 \left[\frac{\Delta \rho g d}{\rho_L} \right]^{1/2}} \quad (19)$$

We note that the relationship (19) usually corresponds to the air void fraction of the Taylor bubble only and not to that of the entire slug unit.

More sophisticated theories have investigated the motion of large gas bubbles rising through liquid flowing in a pipe. *Collins et al.* [1978] incorporated a dependency on the liquid velocity profile in their theoretical treatment, for both laminar and turbulent liquid flow, and found good agreement with the formula (19) for turbulent flow. *Bendiksen* [1985] extended the work of *Collins et al.* [1978] by incorporating surface tension dependency (using the inverse Eötvös number or surface tension number, $\Sigma = \sigma / \rho_L g d^2$, which leads to an extension of the formula (19) within a certain range of Σ . The resulting coefficients C_0 and C_2 will thus depend on Reynolds and inverse Eötvös numbers. *Kelessidis and Dukler* [1990] developed a model for the rise velocity of an elliptic bubble rising through a stagnant liquid in a concentric annulus. These studies show that the formula (19) may be used as a good approximation for the air void fraction in slug flow.

To account also for the difference in the drift flux between the liquid slug and the Taylor bubble, a number of hydrodynamic models have been investigated [*Caetano et al.*, 1992b; *Issa and Tang*, 1990; *Barnea*, 1990; *Fernandes et al.*, 1983]. They are widely known as "two-fluid" models and incorporate the slug structure model to predict the average gas void fraction. *Issa and Tang* [1990] found that the comparison to the drift-flux model show good agreement for low test pressures on the order of 2.46 MPa or less. At higher pressures, their two-fluid model gives better results than the drift-flux model. *Hasan and Kabir* [1992] proposed a hybrid two-fluid model/drift-flux model to calculate the gas void fraction in annuli for slug flow. As we consider only low pressures, we do not apply the two-fluid models, which will lead to more complicated expressions. Rather we estimate the gas void fraction using the basic drift-flux model (19).

Without an annulus, slight differences in the values of C_0 and C_2 are presented in the review of *Sylvester* [1987]. The presence of an annulus in the inner well, represented in our experimental system by the area between the air line and the inner well, forced us to further modify the values of C_0 and C_2 .

The simplest modification would consist of expressing the coefficients C_0 and C_2 as a function of the ratio of the air line diameter to the inner well diameter: the most common modifications found in the literature are listed in the appendix. However, we will propose new expressions for C_0 and the drift velocity V_{drift} through evaluation of our lab data. This is the purpose of section 6.

Our model builds on the modified Clark and Dabolt model. In this new model we always take into account the inertial energy terms, presented in (6), in determining the air-lift pumping operating curve, even though at low flow rates the kinetic energy effects could be neglected. In addition, the friction factor is expressed as a function of the Reynolds number, even though at low flow rates it can be taken as a constant.

5. Operating Curves for Air-Lift Pumping: Behavior of Models

The purpose of this section is to define key terminology used in air-lift pumping and to inspect the behavior of our model, as well as others, over a wide range of air and water flow rates. We base our discussion on the conditions of our laboratory experiments; however, the simulations shown exceed the range of flow rates that we observed in the laboratory.

The operating curve for air-lift pumping is the plot of the injected air flow rate, Q_G , versus the pumping water flow rate, Q_L , for fixed submergence and lift, as in Figure 4a. As air is injected the water begins to respond. Initially, no water flow up the well takes place until a certain air injection rate is reached. This is because the water level in the inner well does not exceed the delivery height $H = L + S$, lift plus submergence. Once the air flow rate exceeds its critical value, noted as Q_{G-min} , the discharge or water flow rate increases rapidly with increasing air flow rate, until a maximum water flow rate is reached. The maximum discharge is labeled "maximum capacity" in Figure 4a. After reaching the maximum the discharge decreases with further increases in the air injection rate.

The physical explanation for the shape of the operating curve relies upon the dominant terms in the momentum equation (6). As air is initially injected, the mixture density decreases, and gravity forces the mixture up the well. In this state the third term, the gravitational term, dominates because the velocity is small and the sum of inertial energy plus frictional terms is negligible. The dominance of the gravitational term continues until the maximum capacity is reached. As the velocity increases further, the velocity dependent terms (hydraulic losses) grow. Beyond the maximum capacity the hydraulic losses overwhelm the gravitational terms, and an increase in air flow rate no longer results in an increase in the liquid flow rate.

The air-lift pumping system also may be characterized by its efficiency, η , defined as the net work done to lift the liquid, divided by the work done by the isothermal expansion of air [*Richardson and Higson*, 1962]:

$$\eta = \frac{Q_L S \rho_L g}{Q_G P_{atm} \ln \left(\frac{P_{sparger}}{P_{atm}} \right)} \quad (20)$$

Figure 4b shows a typical air-lift pumping efficiency curve. It is a plot of the water-to-air ratio, a value proportional to η in (20), plotted against the air flow rate, which is proportional to the energy input from air injection. With increasing air flow rate, the water-to-air ratio increases sharply to the point of

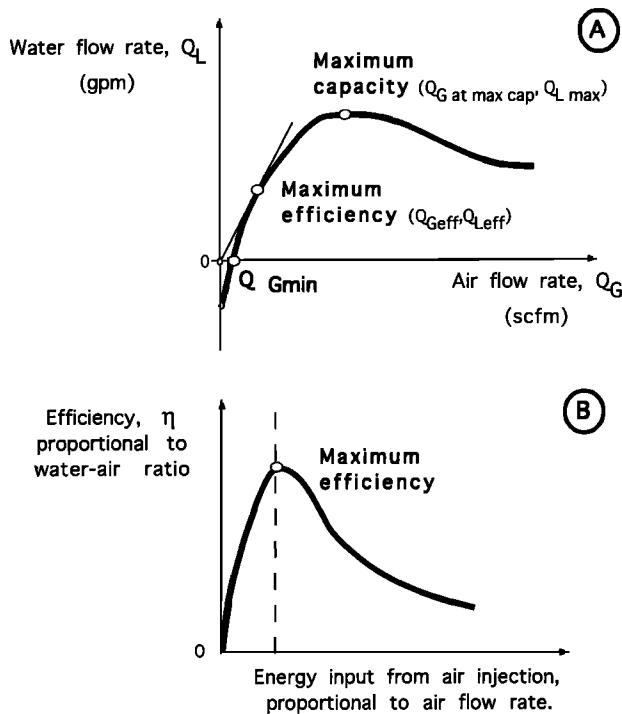


Figure 4. (a) Air-lift pump operating curve and (b) air-lift pump efficiency curve.

maximum efficiency. For a fixed submergence and lift the maximum efficiency corresponds to the lowest air-to-water ratio and is the tangent point on the operating curve, Figure 4a. Our laboratory test conditions are such that the efficiencies of the air-lift pumping system ranges from 9 to 82% and are always

below the point of maximum efficiency, which is thus greater than 82% (to the left of the maximum efficiency point in Figure 4b).

We now compare the results of our new model to the models of Ingersoll and Rand, and Clark and Dabolt for a wide range of air injection rates. The models of Ingersoll and Rand, and Clark and Dabolt, reviewed in section 2, predict different operating curves, which can differ substantially at high flow rates. This is shown in Figure 5 in which we also show our model for two different cases. The upper curve, labeled “modified model,” is for the case of a friction factor that varies dynamically with the Reynolds number, while the lower curve is the new model with a constant friction factor. These curves are for the conditions of the lab configuration with a submergence of 45 feet (13.7 m) and a lift of 20 feet (6.1 m). The three main conclusions drawn from Figure 5 are as follows: (1) The Ingersoll and Rand formula is only valid at maximum efficiency and therefore predicts the lowest air-to-water ratio. (2) In comparing the Clark and Dabolt model with the new model, assuming a constant friction factor, one can see a discrepancy at higher air flow rates. The primary difference between the two models is the inclusion of inertial energy terms in the new model, which are ignored in the Clark and Dabolt model. The effect of the inertial energy terms is to create greater head losses and therefore reduce the water flow rate. (3) We compare the modified Clark and Dabolt model, into which we inserted a friction factor that is a function of the Reynolds number, with the same model containing a constant friction factor. The value of the constant friction factor was 0.01, while the average value of the functional friction factor was about 0.005. We note that the maximum capacity attains a higher value and the maximum is reached with a lower air injection

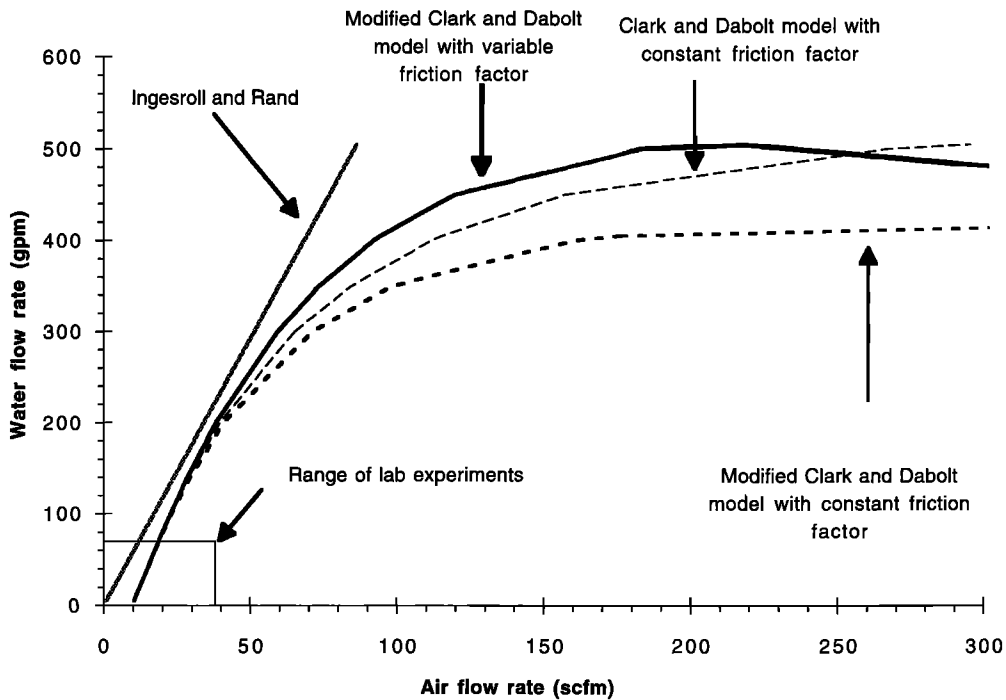


Figure 5. Comparison of Ingersoll and Rand formula, Clark and Dabolt model, and the modified Clark and Dabolt model. The conditions for the simulation are based on the lab setup with $S = 45$ feet (13.7 m) and $L = 20$ feet (6.1 m).

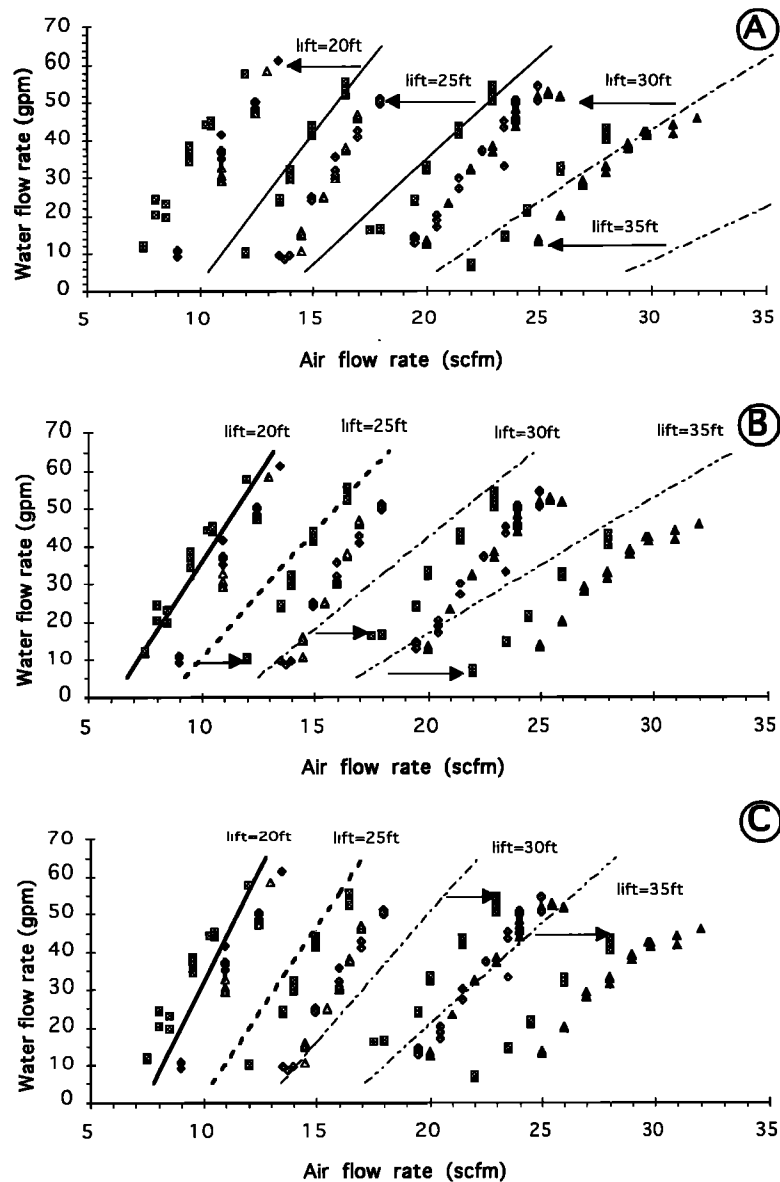


Figure 6. Predictions using the new model for the experimental conditions with the sparger 5 feet (1.5 m) above the bottom of the well. (a) $C_0 = 1.2$ and $C_2 = 0.345$, as in the Clark and Dabolt model. (b) $C_0 = 1.094$ and $C_2 = 0.23$. (c) $C_0 = 0.915$ and $C_2 = 0.3$. The squares represent one set of experiments. The triangles and the diamonds are two repetitions of the experiments. The experimental error is represented by the scatter shown for a particular lift.

rate. This is explained by the value of 0.01 for the friction factor which is a clear overestimate of the true value.

6. Model Comparisons to Laboratory Experiments

The new model was run for the conditions of our laboratory experiments. Only the experiments with the sparger fixed at 5 feet (1.5 m) above the bottom of the well will first be considered. The other experiments will be used for validation. Our laboratory data represent the range of flow rates in the operating curve from 5 to 70 gallons/min (0.32–4.4 L/s), which is below the maximum efficiency point. Over this range of exper-

imental flow rates, neither the change in the friction factor, nor the kinetic energy effects have any significant influence. Therefore the new model is comparable to the Clark and Dabolt model. If the usual drift-flux coefficients are used, $C_0 = 1.2$ and $C_2 = 0.345$ (which leads to $V_{\text{drift}} = 43.31$ cm/s (17.1 inches)), as in the model of Clark and Dabolt, predictions do not match the experimental data. As seen in Figure 6a, the predictions are shifted to the right compared to our data. That is, for a given water flow rate, the model overestimates the required air flow rate by about 5 to 10 standard cubic feet/min (0.14–0.28 m³ STP/min), which corresponds of an error of up to 50%.

To further evaluate the efficacy of the new model, the constants C_0 and C_2 of the drift flux model were systematically

varied. First we grouped all of the data from all experiments over the range of lifts from 20 to 35 feet (6.1–10.7 m). We then determined the least squares/best fit values for the drift-flux coefficients based on (14). The best fit values were $C_0 = 1.094$ and $C_2 = 0.23$ (or $V_{\text{drift}} = 28.87$ cm/s (11.4 inches/s)). It is important to note that this procedure required us to assume a constant average air void fraction, ε , over the entire height of the well as shown in (13). Using these values, the match is generally quite poor (Figure 6b), with a noticeable shift to the left for the predictions compared to the laboratory data. The only exception to this trend is the simulation corresponding to the experiments for the lowest lift, 20 feet (6.1 m). Second, we determined four distinct best fit values of C_0 and C_2 for each of the four experimental lifts. These were then averaged to obtain values of $C_0 = 0.915$ and $C_2 = 0.3$ (or $V_{\text{drift}} = 37.68$ cm/s (14.8 inches/s)). Results using these values of the drift flux coefficient are displayed in Figure 6c. In general, the simulated values are shifted to the left relative to our data, with better agreement only for the low lift experiments, at 20 and 25 feet (6.1 and 7.6 m).

The failure of this new model, which is a modified Clark and Dabolt model, led us to conduct a series of sensitivity analyses to determine the influence of the drift flux coefficients on the position and slope of the operating curves. Our analysis indicated the following: (1) C_0 is the primary control on the slope. Furthermore, when its value decreases, the operating curves are shifted to the left. (2) Increasing C_2 will result in shifting the operating curve to the right. (3) The sensitivity to these drift-flux constants is more important at higher lift or lower submergence. (4) None of these adjustments are able to represent the experimental data at low water flow rates, with lifts higher than 25 feet (7.6 m).

Over the range of the lab test values, where the percentage of submergence varies, and when churn flow occurs, a simple drift-flux expression is not appropriate. When evaluating C_0 and C_2 , or V_{drift} , by comparison with the experimental data, we noticed that C_0 exhibits no obvious dependency on velocities, average void fraction, or pressure. Its value is between 0.68 and 0.95. We note that *Bendiksen* [1985] argued that C_0 is a decreasing function of the Reynolds number. We did not find such a relationship in our analysis for our laboratory conditions. C_2 was dependent upon the average void fraction or percent of submergence, and increased to a constant value following a relationship of the form $1 - \exp[f(\alpha)]$. The range of C_2 values is 0.21 to 0.40, which corresponds to V_{drift} ranging from 26 to 50 cm/s (10.2–19.7 inches/s).

Our expression of the drift-flux velocity V_{drift} , or corresponding C_2 , is based on our analysis of the experimental results coupled with physical reasoning. At a low mixture velocity, which corresponds to a higher percentage of submergence and to a lower average gas void fraction, the Taylor bubbles and slug flow are not well developed. In this case the drift flux velocity can be represented by the terminal bubble rise velocity, V_{bs} . At a higher mixture velocity (lower percentage of submergence or higher average gas void fraction), the Taylor bubbles and slug flow are well developed, and the drift velocity can be represented by the Taylor bubble velocity, V_{tb} . As the bubble/slug transition occurs when the average gas void fraction is around 0.25 [*Taitel et al.*, 1980], or $\alpha = 75\%$, we propose the following formula, for which $25\% < \alpha < 75\%$:

$$V_{\text{drift}} = (V_{\text{tb}} - V_{\text{bs}}) \left(1 - \exp \left[\frac{1 - \alpha - 0.25}{0.06} \right] \right) + V_{\text{bs}} \quad (21)$$

$$C_2 = \frac{V_{\text{drift}}}{\left[\frac{\Delta \rho g d}{\rho_L} \right]^{1/2}} \quad (22)$$

In using the relationships (21) and (22), it can be seen that when the average void fraction is 0.25, then $\alpha = 75\%$, and V_{drift} equals the terminal bubble rise velocity, V_{bs} . Approaching the other extreme, when the average void fraction is greater than 0.45, then $25\% < \alpha < 55\%$, and the value of V_{drift} approaches the Taylor bubble velocity, V_{tb} .

Because C_0 does not follow any particular trend, a constant value was found by matching the experimental data for two sets of runs. For the first set, C_0 varied between 0.78 and 0.96, and for the second set, the values ranged from 1.18 to 0.94. Although there is a wide range of values, we consider C_0 as a constant equal to the average value for the two sets. The new constant C_0 for this experimental annulus configuration where $d_i = 14.07$ cm (5.5 inches) and $d_o = 3.33$ cm (1.3 inches), and with the flow conditions where $2 \text{ cm/s} < W_L < 29 \text{ cm/s}$ and $13 \text{ cm/s} < W_G < 68 \text{ cm/s}$ ($0.8 \text{ inches/s} < W_L < 11.4 \text{ inches/s}$ and $5.1 \text{ inches/s} < W_G < 26.8 \text{ inches/s}$), is

$$C_0 = 0.95 \quad (23)$$

The relationships (21) and (23) were based on the laboratory data for which the sparger was 5 feet (1.5 m) above the bottom of the well. They were validated using the lab test data for which the sparger was moved 25 feet (7.6 m) above the bottom of the well. Using these relationships, the new model was labeled the Stanford model in Figures 7a and 7b. Good agreement was found for the operating curves predicted by the Stanford model and the experimental data, with the higher sparger elevation. Results are shown in Figures 7a and 7b.

To summarize, we propose these relationships:

$$C_0 = 0.95 \quad (23)$$

with $d_o/d_i = 3.33/14.07$,

$$1.1 < C_0 < 1.2 \quad (24)$$

when $d_o = 0$, and, again, (21) and (22):

$$V_{\text{drift}} = (V_{\text{tb}} - V_{\text{bs}}) \left(1 - \exp \left[\frac{1 - \alpha - 0.25}{0.06} \right] \right) + V_{\text{bs}}$$

$$C_2 = \frac{V_{\text{drift}}}{\left[\frac{\Delta \rho g d}{\rho_L} \right]^{1/2}}$$

7. Comparison Between Stanford Model and Other Experimental Data

To explore the validity of our model beyond the conditions of the experiments, we compared it to data presented in the literature. The conditions of each experiment for water pumping by air-lift operations are shown in Table 2. They are sorted by increasing diameter and total length. As can be seen, there are few experiments in our range. The two experiments that are somewhat comparable are those presented by *Clark and Dabolt* [1986] and *Alimonti and Galardini* [1992].

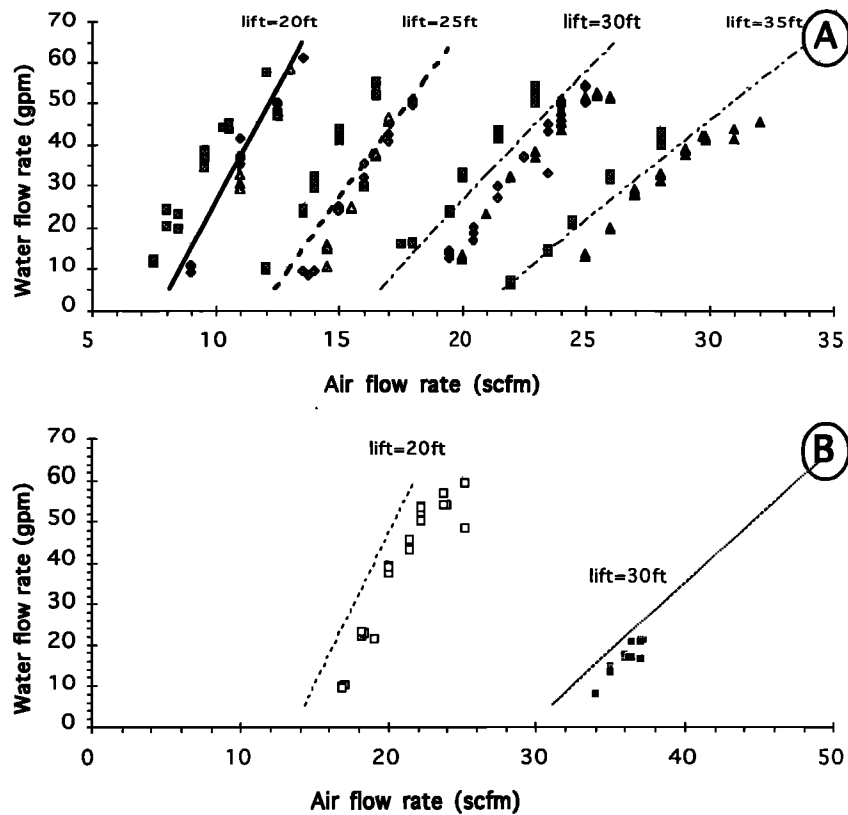


Figure 7. Predictions of the Stanford model for the experimental data. (a) The sparger is 5 feet (1.5 m) above the bottom of the well. (b) The sparger is 25 feet (7.6 m) above the bottom of the well. The squares represent one set of experiments. The triangles and diamonds represent two repetitions of the experiments.

Table 2. Conditions for Experimental Data Presented in the Literature

Authors	Well Diameter d , mm	Total Length $H = L + S$, m	Percent Submergence S	Maximum Liquid Velocity* W_L , cm/s	Maximum Air Velocity* W_G , cm/s
<i>Conditions comparable to our experiments</i>					
Alimonti and Galardini [1992]	26	7.25	60	70	265
Clark and Dabolt [1986]	38.1	15	82	80	50
François et al. (present study)	140.7	13.7, 19.8	33–70	29	68
<i>Conditions not comparable to our experiments</i>					
Jeelani et al. [1979]	2–3.5	1.21–1.30	10–90	50	260
Apazidis [1985]	13	0.49	45–73	37	43
Reinemann et al. [1990]	3.18–19.1	1.8	47–98		20
Stenning and Martin [1968]	25.4	4.27	44.2–70.7	100	1000
Richardson and Higson [1962]	25.4	13.77	50	50	336
Govier et al. [1957]	26	6.97	24–90	225	843
Wang and Chen [1979]	30	4.65	75.3	75	500
Morrison et al. [1987]	38.1	3.04	68.75	200	61
Todoroki et al. [1973]	28.3, 50.6	7.5, 6.8	30–80	170	850
Govier and Short [1958]	16–63.5	6.97	47–84	106	456
Moore and Wilde [1931]	25.4–101.6	20.5	3.6–96.5	142	1561
Shaw [1920]	127	138–174	29–47	165†	2575†
Parker and Suttle [1987]	37.5–300	0.15–1.20	100	16	20

*Liquid velocity and air velocity are the superficial velocities, as defined by (2c).

†The data of the Shaw experiments are primarily in the annular flow regime.

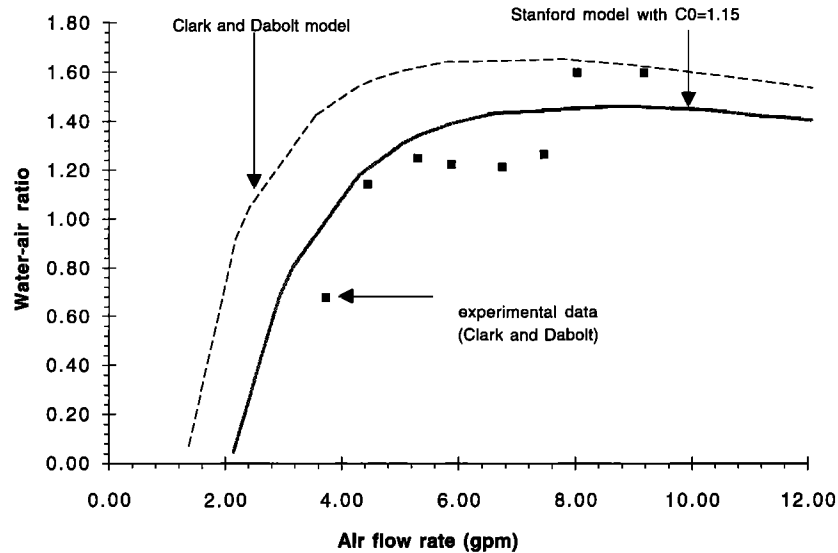


Figure 8. Comparison between the Stanford model and the Clark and Dabolt model for the data presented by Clark and Dabolt [1986].

7.1. Clark and Dabolt Experiment, or Average Air-Lift System

The air-lift installation described by Clark and Dabolt is similar to the conditions of our laboratory experiments. Their total well length was $H = 15$ m (49.2 feet), versus ours of 13.7 and 19.8 m (45 and 65 feet); their well diameter was $d_i = 3.81$ cm (1.5 inches), versus ours of 14.07 cm (5.5 inches). For a submergence ratio of 82%, air-lift operations were below the maximum efficiency, with efficiency ranging from 23 to 53%, and with a liquid-to-gas ratio up to about 1.6. This compares with our experiments, in which the submergence ratio ranged from 33 to 70%, with a liquid-to-gas ratio up to 0.7 and with efficiency ranging from 9 to 82%. Figure 8 shows the comparisons between the Clark and Dabolt data and our respective models. C_2 was calculated using (21) and (22) and had a value of 0.471. C_0 was set equal to 1.15. This value was selected to be greater than the value used in our experimental setup because their setup had no internal air line (no annulus), and their well diameter was about 25% of ours. We note that the value of 1.2 selected for C_0 is close to the value suggested by Clark and Dabolt. Our model results agree nicely with their experimental data.

7.2. Alimonti and Galardini Experiment, or Small Air-Lift System

The experiment described by Alimonti and Galardini [1992] is a small air-lift system (diameter of 2.6 cm (1.0 inch), total length of 7.25 m (23.8 feet), and a percentage of submergence of 60%). Most of the experimental points are near the maximum efficiency point or above. When adjusting C_0 in our model to fit these experimental conditions, the best fit for the points below maximum efficiency was given with $C_0 = 1.1$. The model determined $C_2 = 0.37$. Figure 9 shows the Alimonti and Galardini experimental data as well as the predictions of the respective models. For the highest flow rates, neither model accurately fits the experimental data. Because we are most concerned with the points corresponding to air flow rates less than the point of maximum efficiency, our model fit in this range is superior to that of Alimonti and Galardini.

8. Model Parameter Sensitivity Analysis

A model parameter sensitivity analysis was conducted around those parameters fit to our laboratory data, for the conditions of submergence of 40 feet (12.3 m), lift of 25 feet (7.6 m), water flow rate of 24.6 gallons/min (1.55 L/s), and predicted air flow rate of 14.7 standard cubic feet/min (0.42 L/s). We varied each parameter by $\pm 10\%$ and noted the relative change in the air flow rate. In addition, we inspected the relative change in both the maximum efficiency and maximum capacity resulting from parameter changes of $\pm 10\%$.

The relative change in the gas flow rate as a function of a change in one parameter is defined as R_G :

$$R_G = \frac{Q_G^* - Q_G}{Q_G} \quad (25)$$

where the asterisk denotes a value of Q_G with the $\pm 10\%$ variation of the parameter.

The results are presented in Figure 10. Several key points can be made by inspecting the figure. First, the primary control on the sensitivity of air flow rate is the inner well diameter, d_i , which generates R_G values of ranging from ± 18 to $\pm 29\%$. Second, changing the submergence, S , by $\pm 10\%$ causes a change in the operating air flow rate of about 10%, but causes a change of up to 25% in the maximum capacity. Third, there are five parameters (the discharge pressure, P_{top} ; the acceleration of gravity, g ; the lift, L ; and the drift coefficients, C_0 and C_2) that cause less than a 10% change in the air flow rate. Fourth, there are six parameters (temperature, T ; water density, ρ_L ; water flow rate, Q_L ; air line diameter, d_o ; frictional parameter, n ; and friction factor, f) that generate less than a 3% change in R_G . Although some of these parameters, such as pipe and air line diameters, are generally accurately known, others, such as water flow rate, temperature, and discharge pressure, are less precisely known. The parameters that cannot be directly measured are the frictional parameter, the friction factor, and the two drift-flux coefficients. Changes in the former coefficients are inconsequential to the predicted air flow rate, while the latter are important. Of all of the impre-

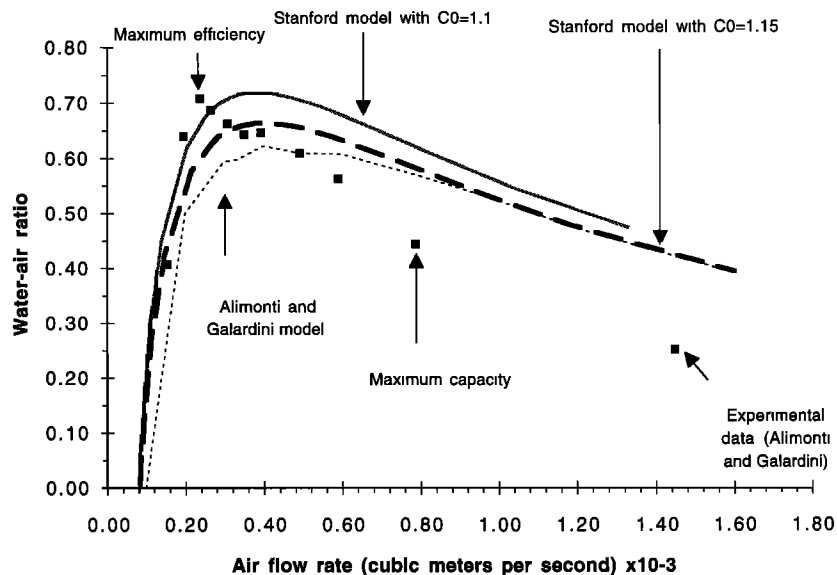


Figure 9. Comparison between the Stanford model and the Alimonti and Galardini model for the Alimonti and Galardini [1992] data.

cisely known parameters, the ones that have the greatest influence are the discharge pressure and the drift coefficients. In many cases it is logical to assume that the discharge pressure is atmospheric. However the drift-flux coefficients, C_0 and C_2 , are never well known. One contribution of our model is to better define the drift-flux coefficient C_2 .

9. Conclusion

We conducted a series of full-scale air-lift pumping experiments in the laboratory. Our aim was to observe the regimes of air flow and to evaluate existing expressions for air-lift pumping. Because of the inability of previous air-lift pumping sim-

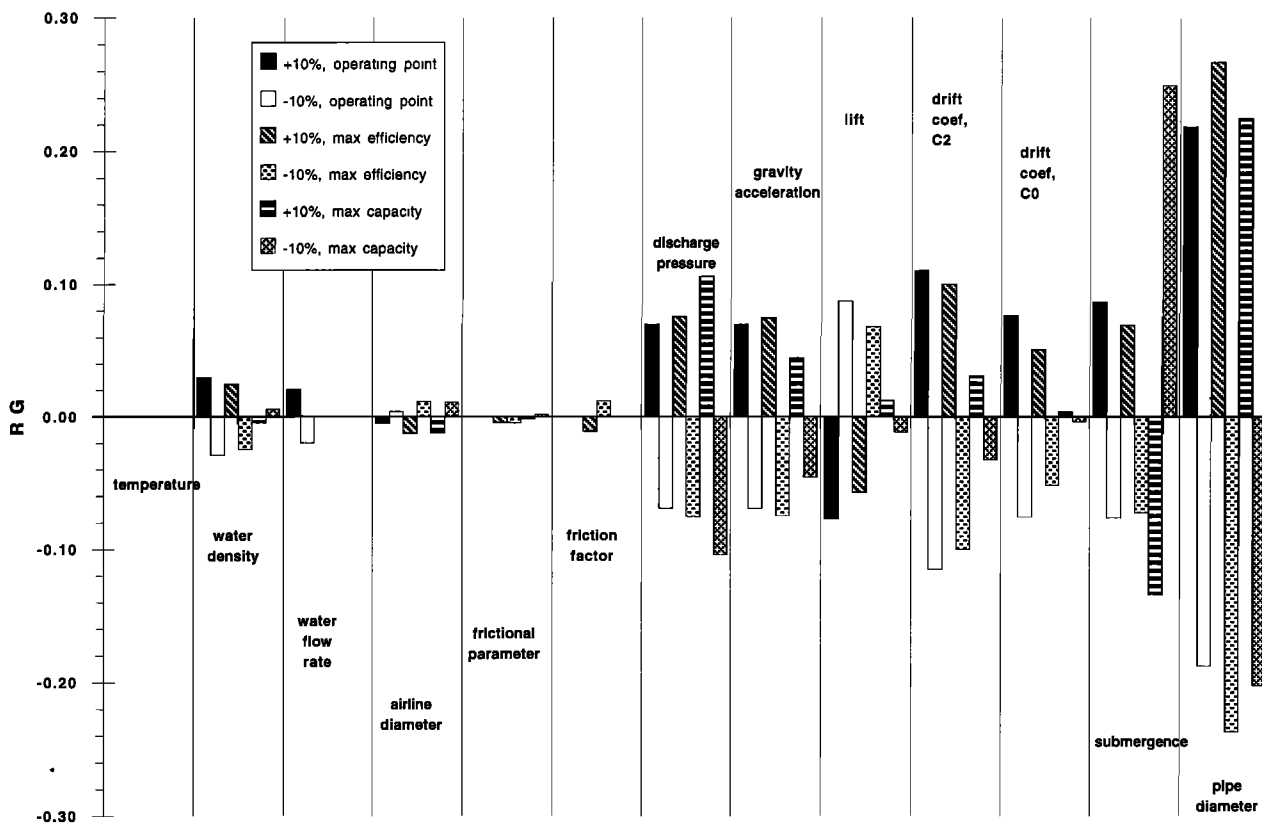


Figure 10. Model parameter sensitivity analysis showing a change in the air flow rate due to a 10% change in each parameter. The starting conditions for this sensitivity study are $S = 40$ feet (12.2 m), $L = 25$ feet (7.6 m), $Q_L = 24.6$ gallons/min (1.55 L/s), and $Q_G = 14.7$ standard cubic feet/min (0.41 m³ STP/min).

ulation models to reproduce our laboratory data, we developed a new relationship. We suggest the use of our model for the operating conditions: (1) at flow rates less than the point of maximum efficiency; (2) with inner well diameters between 4 and 10 inches (10 to 25 cm); and (3) with percentages of submergence between 30 and 70%, which in many practical cases of in-well air stripping corresponds to air-to-water ratios between about 2 and 30.

Comparisons between our laboratory data and the model of Clark and Dabolt indicated that in this flow regime their model is inapplicable. Specifically, their model is appropriate for wells of very small diameters, perhaps less than 3 inches (7.5 cm), and a large percent of submergence. Use of the Clark and Dabolt model tends to overpredict the water flow rate resulting from a given air flow rate, even for their own experiments (see Figure 8). For our experiments, in which the percent submergence is only about 50% (compared to their 82%), using the Clark and Dabolt model tends to underpredict the water flow rate resulting from a given air flow rate, and becomes worse with increasing lift.

We developed a model for the range of our experimental conditions that adds the following features to the original model of Clark and Dabolt: (1) the drift flux coefficient C_2 is now represented by a function of the percent submergence; (2) the friction factor is a dynamic function of the Reynolds number; and (3) inertial energy terms are included in the model, thereby accounting for head losses due to gas expansion, which causes the water to accelerate.

This new model matches the operating curves for the six experiments that we have conducted, over a range of lifts and submergences. In addition, our model matches the data presented by Clark and Dabolt [1986] and by Alimonti and Galar-dini [1992]. Although our model was quite successful in matching these experimental data, it is restricted to air flow rates less than the maximum efficiency. We suspect that a more complex relationship for the frictional losses than the linear form we have employed, would further improve the applicability of our model. Performance of this under field conditions will be part of ongoing demonstrations and applications of the in-well air stripping approach for removing VOCs from groundwater.

Appendix

Ingersoll and Rand Formula

Gibbs [1971, chap. 31, p. 7] reported that "an empirical formula for free air quantity in cubic feet per gallon of water pumped, V_a , has been developed from many tests. This may be used for preliminary estimating." This is the usual Ingersoll and Rand formula:

$$V_a = \frac{L}{C \log_{10} \frac{S + 34}{34}}$$

with S and L in feet. The constant C is given graphically as a function of the percentage of submergence. This formula is only applicable for conditions of maximum efficiency, and will plot as a horizontal line on Figure 4b.

Zenz Formula

Zenz [1993] proposed a general correlation based on published air-lift data. This correlation is a mean curve where the ordinate is

$$Y = \frac{Q_L}{A} \left(\frac{48L}{d_o} \right) 0.5 / \frac{\rho_m}{62.4} \log_{10} \left(\frac{S + 34}{34} \right)$$

and the abscissa is

$$X = \frac{Q_G}{A} \left(\frac{48\rho_G}{d_i L \rho_m} \right)^{0.5}$$

In this formula, Q_L is in gallons per minute, A is in square feet, L and S are in feet, d_i is in inches, and ρ_m and ρ_G are in pounds per cubic foot. The Zenz formula is particularly valuable at high superficial velocities.

Fanning Friction Factor Formula

The two-phase flow friction factor expressions proposed by Caetano *et al.* [1992a] depend on the flow regime: laminar flow and turbulent flow, determined through the Reynolds number of the mixture. The mixture Reynolds number is given by

$$Re = \frac{\rho_m W_m (d_i - d_o)}{\mu_m}$$

with μ_m , the mixture viscosity, given by

$$\mu_m = \varepsilon \mu_G + (1 - \varepsilon) \mu_L$$

For laminar flow, the Fanning friction factor in circular pipe, f_{lam0} , is inversely proportional to the Reynolds number, Re :

$$f_{lam0} = \frac{16}{Re}$$

For a concentric annulus, where $K = d_o/d_i$, $\pi > 0$, this factor is

$$f_{lam} = \frac{F(K)}{Re}$$

with

$$F(K) = \frac{16(1 - K^2)}{\left[\frac{1 - K^4}{1 - K^2} - \frac{1 - K^2}{\ln(1/K)} \right]}$$

In turbulent flow, the Fanning friction factor is defined as the solution of the equation

$$\begin{aligned} & 1 / \left\{ \left(f \left[\frac{16}{F(K)} \right] \right)^{0.45 \exp[-(Re-3000)/10E+06]} \right\}^{1/2} \\ & = 4 \log \left\{ Re \left(f \left[\frac{16}{F(K)} \right] \right)^{0.45 \exp[-(Re-3000)/10E+0.6]} \right\}^{1/2} - 0.4 \end{aligned}$$

Effect of Annular Dimension on C_0 and C_2 Values

Here we review all the formulas for the drift flux parameters C_0 and C_2 presented in the literature.

Caetano *et al.* [1992a] proposed the following relationship for C_2 and V_{tb} :

$$C_2 = 0.345 \left(1 + \frac{d_o}{d_i} \right)$$

$$V_{tb} = 0.345 \left[1 + \frac{d_o}{d_i} \right] [gd_i]^{0.5}$$

Kabir and Hasan [1990] proposed these values:

for slug flow

$$C_0 = 1.18 + 0.9 \frac{d_o}{d_i}$$

for churn flow

$$C_0 = 1.15$$

$$V_{tb} = \left[0.3 + 0.22 \frac{d_o}{d_i} \right] \left[g(d_i - d_o) \frac{\Delta\rho}{\rho_L} \right]^{0.5}$$

These formulas were modified by *Hasan and Kabir* [1992], with for slug flow

$$C_0 = 1.2$$

for churn flow

$$C_0 = 1.15$$

$$V_{tb} = \left[0.345 + 0.1 \frac{d_o}{d_i} \right] \left[g d_i \frac{\Delta\rho}{\rho_L} \right]^{0.5}$$

Acknowledgments. We are most thankful to Ghislain de Marsily for his thoughtful review comments. We gratefully acknowledge the support of the DOE through the arid zone VOC integrated demonstration program administered through the Western Region Hazardous Substance Research Center. We also thank NSF for their support through grant BCS-8957186 and the Hewlett-Packard Company for their grant of computer equipment.

References

- Alimonti, C., and D. Galardini, The modeling of an air-lift pump for the design of its control system, *Eur. J. Mech. Eng.*, 37(3), 191–197, 1992.
- Apazidis, N., Influence of bubble expansion and relative velocity on the performance and stability of an airlift pump, *Int. J. Multiphase Flow*, 11(4), 459–479, 1985.
- Barnea, D., Effect of bubble shape on pressure drop calculations in vertical slug flow, *Int. J. Multiphase Flow*, 16(1), 79–89, 1990.
- Bendiksen, K. H., On the motion of long bubbles in vertical tubes, *Int. J. Multiphase Flow*, 11(6), 797–812, 1985.
- Bilicki, Z., and J. Kestin, Transition criteria for two-phase flow patterns in vertical upward flow, *Int. J. Multiphase Flow*, 13(3), 283–294, 1987.
- Caetano, E. F., O. Shoham, and J. P. Brill, Upward vertical two-phase flow through an annulus, I, Single-phase friction factor, Taylor bubble rise velocity, and flow pattern prediction, *J. Energy Res. Technol.*, 114, 1–13, 1992a.
- Caetano, E. F., O. Shoham, and J. P. Brill, Upward vertical two-phase flow through an annulus, II, Modeling bubble, slug and annular flow, *J. Energy Res. Technol.*, 114, 14–30, 1992b.
- Clark, N. N., and R. J. Dabolt, A general design equation for air-lift pumps operating in slug flow, *AIChE J.*, 32(1), 56–64, 1986.
- Collins, R., F. F. De Moraes, J. F. Davidson, and D. Harrison, The motion of a large gas bubble rising through liquid flowing in a tube, *J. Fluid Mech.*, 89(3), 497–514, 1978.
- Fernandes, R. C., R. Semiat, and A. E. Dukler, Hydrodynamic model for gas-liquid slug flow in vertical tubes, *AIChE J.*, 29(6), 981–989, 1983.
- Gibbs, C. W., Air lift pumping in *Compressed Air and Gas Data*, 2nd ed., pp. 31–1–31–14, Ingersoll-Rand, Woodcliff Lake, N. J., 1971.
- Govier, G. W., and K. Aziz, *The Flow of Complex Mixtures in Pipes*, Van Nostrand Reinhold, New York, 1972.
- Govier, G. W., and W. L. Short, The upward vertical flow of air-water mixtures, II, Effect of tubing diameter on flow pattern, holdup, and pressure drop, *Can. J. Chem. Eng.*, 36, 195–202, 1958.
- Govier, G. W., B. A. Radford, and J. S. C. Dunn, The upwards vertical flow of air-water mixtures, I, Effect of air and water-rates on flow pattern, holdup, and pressure drop, *Can. J. Chem. Eng.*, 35, 58–70, 1957.
- Grandjean, B. P. A., F. Ajersch, P. J. Carreau, and I. Patterson, Study of an air-lift system, I, Hydrodynamics of the Atara piston bubble canon mixer, *Can. J. Chem. Eng.*, 65, 430–436, 1987.
- Gvirtsman, H., and S. M. Gorelick, The concept of in-situ vapor stripping for removing VOCs from groundwater, *Transp. Porous Media*, 8, 71–92, 1992.
- Gvirtsman, H., and S. M. Gorelick, Using air-lift pumping as an in-situ aquifer remediation technique, *Water Sci. Technol.*, 27(8), 195–201, 1993.
- Harmathy, T., Velocity of large drops and bubbles in media of infinite and of restricted extent, *AIChE J.*, 6, 281, 1960.
- Hasan, A. R., and C. S. Kabir, A study of multiphase flow behavior in vertical wells, *SPE Prod. Eng.*, 3, 263–272, May 1988.
- Hasan, A. R., and C. S. Kabir, Two-phase flow in vertical and inclined annuli, *Int. J. Multiphase Flow*, 18(2), 279–293, 1992.
- Hewitt, G. F., and S. Jayanti, To churn or not to churn, *Int. J. Multiphase Flow*, 19(3), 527–529, 1993.
- Husain, L. A., and P. L. Spedding, The theory of the gas-lift pump, *Int. J. Multiphase Flow*, 3, 83–87, 1976.
- Issa, R. I., and Z. F. Tang, Modelling of vertical gas-liquid slug flow in pipes, in *Advances in Gas-Liquid Flows*, Am. Soc. Mech. Eng. Fluids Eng. Div., 65–71, 1990.
- Jayanti, S., and G. F. Hewitt, Prediction of the slug-to-churn flow transition in vertical two-phase flow, *Int. J. Multiphase Flow*, 18(6), 847–860, 1992.
- Jeelani, S. A. K., K. V. Kasipati Rao, and G. R. Balasubramanian, The theory of the gas-lift pump: A rejoinder, *Int. J. Multiphase Flow*, 5, 225–228, 1979.
- Kabir, C. S., and A. R. Hasan, Performance of a two-phase gas/liquid flow model in vertical wells, *J. Pet. Sci. Eng.*, 4, 273–289, 1990.
- Kabir, C. S., and A. R. Hasan, Two-phase flow correlations as applied to pumping well testing, *SPE Pap.*, 21728, 861–872, 1991.
- Kelessidis, V. C., and A. E. Dukler, Motion of large gas bubbles through liquids in vertical concentric and eccentric annuli, *Int. J. Multiphase Flow*, 16(3), 375–390, 1990.
- Lockhart, R. W., and R. C. Martinelli, Proposed correlation of data for isothermal two-phase, two component flow in pipes, *Chem. Eng. Prog.*, 45, 39–48, 1949.
- Mao, Z. S., and A. E. Dukler, The myth of churn flow?, *Int. J. Multiphase Flow*, 19(2), 377–383, 1993.
- Moore, T. V., and H. D. Wilde, Experimental measurement of slipage in flow through vertical pipes, *Trans. Am. Inst. Min. Metall. Pet. Eng.*, 92, 296–308, 1931.
- Morrison, G. L., T. I. Zeineddine, M. Henriksen, and G. B. Tatterson, Experimental analysis of the mechanics of reverse circulation air lift pump, *Ind. Eng. Chem. Res.*, 26, 387–391, 1987.
- Nakazatomi, M., H. Shimizu, T. Ochiai, Y. Kakuno, and K. Sekoguchi, Effect of pressure on void fraction in vertical upward gas-liquid two-phase flow, II, An assessment of published correlations of void fraction through high pressure experimental data and a proposal of a new correlation, *Technol. Rep.* 43, 2158, pp. 277–286, Osaka Univ., Osaka, Japan, 1993.
- Nicklin, D. J., The air-lift pump: Theory and optimization, *Trans. Inst. Chem. Eng.*, 41, 29–39, 1963.
- Nicklin, D. J., J. O. Wilkes, and J. F. Davidson, Two-phase flow in vertical tubes, *Trans. Inst. Chem. Eng.*, 40, 61–68, 1962.
- Parker, N. C., and M. A. Suttle, Design of airlift pumps for water circulation and aeration in aquaculture, *Aquacult. Eng.*, 6, 97–110, 1987.
- Reinemann, D. J., J. Y. Parlange, and M. B. Timmons, Theory of small-diameter airlift pumps, *Int. J. Multiphase Flow*, 16(1), 113–122, 1990.
- Richardson, J. F., and D. J. Higson, A study of the energy losses associated with the operation of an air-lift pump, *Trans. Inst. Chem. Eng.*, 40, 169–182, 1962.
- Shaw, S. F., Unwatering the Tiro general mine by air-lift, *Trans. Am. Inst. Min. Metall. Pet. Eng.*, 62, 421–456, 1920.
- Stenning, A. H., and G. B. Martin, An analytical and experimental study of air-lift pump performance, *J. Eng. Power A*, 90(2), 106–110, 1968.
- Sylvester, N. D., A mechanistic model for two-phase vertical slug flow in pipes, *J. Energy Res. Technol.*, 109, 206–213, 1987.
- Taitel, Y., D. Bornea, and A. E. Dukler, Modelling flow pattern transitions for steady upward gas-liquid flow in vertical tubes, *AIChE J.*, 26(3), 345–354, 1980.

- Todoroki, I., Y. Sato, and T. Honda, Performance of air-lift pump, *Bull. JSME*, 94(16), 733-741, 1973.
- Ueda, T., and Y. Koizumi, Two-phase mixture level swell in vertical pipes, *Int. J. Multiphase Flow*, 19(1), 1-13, 1993.
- Wang, T. S., and C. K. Chen, Study on the performances of air-lift pump, in *Multiphase Transport, Fundamentals, Reactor Safety, and Applications*, vol. 4, edited by T. Nejat Veziroglu, Hemisphere, Washington, D. C., 1979.
- Zenz, F. A., Explore the potential of air-lift pumps and multiphase, *Chem. Eng. Prog.*, 89(8), 51-56, 1993.
- Zuber, N., and J. A. Findlay, Average volumetric concentration in two-phase flow systems, *J. Heat Transfer, C*, 97(4), 453-468, 1965.
-
- O. François, S. Gorelick, and M. J. Pinto, Department of Geological and Environmental Sciences, Stanford University, Stanford, CA 94305-2115. (e-mail: gorelick@geo.stanford.edu)
- T. Gilmore, Pacific Northwest Laboratory, Richland, WA 99352.

(Received June 8, 1995; revised March 13, 1996;
accepted March 18, 1996.)